

Functionalization and use of grape stalks as poly(butylene succinate) (PBS) reinforcing fillers

*Original*

Functionalization and use of grape stalks as poly(butylene succinate) (PBS) reinforcing fillers / Nanni, A.; Cancelli, U.; Montecchi, G.; Masino, F.; Messori, M.; Antonelli, A.. - In: WASTE MANAGEMENT. - ISSN 0956-053X. - 126:(2021), pp. 538-548. [10.1016/j.wasman.2021.03.050]

*Availability:*

This version is available at: 11583/2896103 since: 2021-04-20T16:43:58Z

*Publisher:*

Elsevier Ltd

*Published*

DOI:10.1016/j.wasman.2021.03.050

*Terms of use:*

This article is made available under terms and conditions as specified in the corresponding bibliographic description in the repository

*Publisher copyright*

Elsevier postprint/Author's Accepted Manuscript

© 2021. This manuscript version is made available under the CC-BY-NC-ND 4.0 license  
<http://creativecommons.org/licenses/by-nc-nd/4.0/>. The final authenticated version is available online at:  
<http://dx.doi.org/10.1016/j.wasman.2021.03.050>

(Article begins on next page)

1 **Functionalization and use of grape stalks as poly(butylene succinate) (PBS)**  
2 **reinforcing fillers**

3

4 Alessandro Nanni<sup>a</sup>, Umberto Cancelli<sup>b</sup>, Giuseppe Montevecchi<sup>b,\*</sup>, Francesca Masino<sup>b</sup>,  
5 Massimo Messori<sup>a</sup>, Andrea Antonelli<sup>b</sup>

6

7 <sup>a</sup>Department of Engineering Enzo Ferrari, University of Modena and Reggio Emilia,  
8 Via Pietro Vivarelli 10, Modena, Emilia-Romagna, 41125, Italy

9 <sup>b</sup>Department of Life Sciences (Agri-Food Science Area), BIOGEST - SITEIA  
10 Interdepartmental Centre, University of Modena and Reggio Emilia, Piazzale Europa 1,  
11 Reggio Emilia, Emilia-Romagna, 42124, Italy

12

13

14 Corresponding author: Giuseppe Montevecchi

15 E-mail address: giuseppe.montevecchi@unimore.it (G. Montevecchi).

16

17

18 **ABSTRACT:** Grape stalks are a lignocellulosic biomass, which is a very complex  
19 material, whose easy and profitable fractionation to obtain its basic components is still  
20 not available. Therefore, alternative ways to try and make use of grape stalks are  
21 currently being explored.

22 In the present study, the possible use of dried and milled grape stalks as filler in bio-  
23 composites was assessed using polybutylene succinate as a basic polymer. The tensile  
24 specimens produced using 10% grape stalk powder as it is and functionalized through  
25 pre-extrusion acetylation and silylation, and silylation *in situ* were characterized for  
26 their structural, mechanical, thermal, morphological, and color properties. The bio-  
27 composites showed to be stiffer than the control polymer, with an increase of Young's  
28 modulus from 616 MPa to 732 MPa in the specimens obtained with acetylated grape  
29 stalk powder.

30 This led to a potentially new method to valorize by-products of the wine industry such  
31 as grape stalks in order to recover raw materials which could prove useful in the  
32 biomaterials and bio-composites sector.

33

34 **KEYWORDS:** wine chain; by-product; lignocellulosic biomass; composites;  
35 biopolymers.

36

37

## 38 **1. Introduction**

39 The increase of the world population and the corresponding growth in consumption has  
40 led in recent years to an expansion of industrial activities in order to produce goods and  
41 services, especially in the agro-industrial sector (Brandt et al., 2013, Lieder and Rashid,  
42 2016, Maina et al., 2017, Nanni et al., 2021). This involves the issues of accumulation  
43 and disposal of by-products present at various cycles of the food chain (Gustavsson et  
44 al., 2011).

45 Nowadays, one of the strategies most used to reduce the socio-economic and  
46 environmental impact of by-products in the production chain is the creation of closed  
47 systems (Parisi et al., 2021, Ravindran and Jaiswal, 2016). Indeed, the circular economy  
48 allows by-products, which would otherwise end up as waste, to be converted into  
49 secondary raw materials. In the logic of a regenerative approach, these materials can be  
50 returned to the various production cycles for the creation of value-added products  
51 (MacArthur, 2013, Stegmann et al., 2020).

52 The grapevine is one of the most cultivated crops in Italy and the plains and hills of the  
53 Emilia-Romagna region, in Northern Italy, are particularly devoted to this practice.  
54 Here, grapes are mainly intended for the production of wine, however other products  
55 derived from grapes, such as enocyanin from Ancellotta, vinegar, balsamic vinegar,  
56 concentrated musts, and traditional garnishes contribute to the issue of the accumulation  
57 of by-products (Masino et al., 2008, Montevercchi et al., 2011, Montevercchi et al., 2014,  
58 Vasile Simone et al., 2013).

59 In particular, the management of grape stalks, grape pomace, yeast lees, and wastewater  
60 remains an unsolved problem (Barba et al., 2016, Cancelli et al., 2020). According to  
61 some data deriving from the calculation of the carbon footprint of Italian winemaking,

62 the equivalent CO<sub>2</sub> emissions in 2016 were 834,300 tons for grape pomace and 185,400  
63 for grape stalks (Bevilacqua et al., 2017, Lucarini et al., 2018). These latter are  
64 extraordinarily recalcitrant for employment in convenient applications and, for this  
65 reason, they are still highly underutilized.

66 The presence of resistant fibrous biopolymers in the structure of lignocellulosic biomass  
67 makes it interesting as a reinforcing filler in the realization of bio-composite materials  
68 (Ghaffar et al., 2015, Hernandez Michelena, 2019). Bio-composites produced through  
69 the incorporation of a filler deriving from food by-products into a biodegradable and  
70 biobased polymer are nowadays among the most interesting materials for future  
71 applications in the sector of bioplastics and packaging (Bharath and Basavarajappa,  
72 2016, Fortea-Verdejo et al., 2017, Nanni and Messori, 2020a, Nanni et al., 2020,  
73 Seggiani et al., 2015, Seggiani et al., 2016). In particular, lignocellulosic fibers have  
74 many advantages such as low cost, non-toxicity, biodegradability, and easy availability  
75 (Kalia et al., 2013).

76 Among the most interesting polymers nowadays available in the market, polybutylene  
77 succinate (PBS) is an aliphatic polyester that, thanks to its mechanical properties similar  
78 to the ones of polypropylene and polyethylene (Hernandez Michelena, 2019, Luzi et al.,  
79 2019), can find space in many applications such as agriculture, packaging films, and  
80 consumer's goods. Moreover, PBS is highly sustainable, as its building blocks are  
81 partially bio-based. In the last years, its monomers, namely 1,4-butanediol and succinic  
82 acid, have been synthesized also through fermentation of agro-industrial derived sugars  
83 (Yeh et al., 2010, Yim et al., 2011, Zeikus et al., 1999), and it is also fully  
84 biodegradable; thus, its use could reduce the consumption of fossil fuels and tackle the  
85 problems relating to plastic pollution at the same time. Therefore, the possibility to use

86 grape stalks as PBS reinforcing filler is very intriguing since they would simultaneously  
87 increase the PBS bio-based content and offer a new opportunity of waste valorization to  
88 wine-sector companies.

89 As for possible preliminary treatments to improve the characteristic of the finished  
90 product, chemical functionalization of the grape stalk powder has already been  
91 successfully used to increase the adhesion between the hydrophobic polymer and the  
92 polar lignocellulosic matrix (Abdellaoui et al., 2018, Espert et al., 2003, Gwon et al.,  
93 2010a). Acetylation and silanization are two common techniques to cap hydroxyl  
94 groups and ease the creation of hydrophobic interactions between the functionalized  
95 lignocellulose and the polymer (Gwon et al., 2010a). Furthermore, the functionalization  
96 of the lignocellulosic structure increases its stability against moisture and  
97 biodeterioration (Mohammed-Ziegler et al., 2008).

98 The general aim of this project is to explore alternative solutions for the technical and  
99 commercial valorization of grape stalks. In particular, in the Emilia-Romagna region  
100 where we conducted this study, and specifically in the provinces of Modena and Reggio  
101 Emilia, the amount of grape stalks used for the production of biogas and composted  
102 digestate can be up to 2800 t/year (Ronga et al., 2019). Although grape stalks are  
103 partially used for livestock feeding (Maicas and Mateo, 2020), the highest amount is  
104 either destined to landfills or it is left to accumulate on the soil with consequent  
105 phytotoxicity problems caused by the phenolic compounds to the microbiota (Troncozo  
106 et al., 2019).

107 For these reasons, the purpose of this study is the production and evaluation of grape  
108 stalk powder as a filler for biocomposite production using PBS as a basic polymer.

109 Grape stalks powder was also used in its functionalized forms through acetylation and

110 silanization. The structural, mechanical, thermal, and color properties were measured to  
111 ascertain the potential replacement of a part of PBS in order to obtain the least possible  
112 loss of performance.

113

## 114 **2. Experimental**

### 115 **2.1. Chemicals**

116 Acetic anhydride, ethanol, pyridine, and toluene were supplied by Sigma-Aldrich  
117 (Milan, Italy). The paraffinic oil “Vestan” was provided by Tizi S.r.l. (Arezzo, Italy),  
118 while Geniosil GF 31 3-trimethoxysilylpropyl 2-methylprop-2-enoate (MPTMS, CAS  
119 2530-85-0) came from Wacker Chemical Corporation (Milan, Italy). Deionized water  
120 was obtained through an Elix<sup>3UV</sup> purification system (Merck Millipore, Milan, Italy).

121

### 122 **2.2. Sampling, drying, and milling to obtain a fine powder**

123 Grape stalks (200 kg), collected from some wine cellars in the provinces of Modena and  
124 Reggio Emilia, were first cleaned to remove residues of grape skins and grape seeds and  
125 then oven-dried at 65 °C (24-48 h) up to constant weight. Then, the dried grape stalks  
126 were subjected to milling (universal cutting mill, Pulverisette 19, Fritsch GmbH, Idar-  
127 Oberstein, Germany) in order to considerably reduce the dimensions of the material.  
128 The result obtained was a fine powder with a high surface area, thus facilitating the  
129 subsequent treatments of the material. The powder was then sieved to separate it into  
130 the following mesh classes: 63 µm, 212 µm, 500 µm, and 850 µm. The various sieves  
131 (Giuliani Tecnologie S.r.l., Torino, Italy) were stacked in decreasing order of mesh size.  
132 The powder was placed on the first sieve with a mesh size of 850 µm and through a  
133 vibratory movement the various fractions separated and settled down on different levels

134 according to the particle size. The fraction of the powder taken into consideration for  
135 the realization of bio-composite materials was that of a particle size between 63 and 212  
136  $\mu\text{m}$ .

137

### 138 ***2.3. Functionalization through acetylation***

139 This fraction was subjected to an acetylation reaction (Fig. S1a) and an aliquot of 50.00  
140 g of the powder was weighed and introduced into a 1-L flask with 500 mL of acetic  
141 anhydride and 50 mL of pyridine (Hussain, 2004). The reaction flask was immersed in a  
142 silicone oil bath under continuous stirring for about 3 h at 160 °C. The material was  
143 then filtered by the Büchner apparatus and thrice washed with 30 mL of ethanol to  
144 remove the reagents. The solid residue recovered was dried in a stove at 65 °C for two  
145 days.

146

### 147 ***2.4. Functionalization through silanization***

148 The same fraction of powder was subjected to the silanization reaction with MPTMS as  
149 a derivatizing reagent (Fig. S1b) to modify the lignocellulose structure by forming C-O-  
150 Si ester bonds (Abdellaoui et al., 2018, Hernandez Michelena, 2019). An aliquot of  
151 25.00 g of grape stalk powder was dispersed in 25.00 g of toluene and 24.84 g of  
152 MPTMS was added to this mixture (Brostow et al., 2016). The sample was then washed  
153 with toluene and filtered by a Büchner funnel and the solid residue recovered from this  
154 mixture was dried at 70 °C for 24 h. The yields of the two reactions were determined.

155

### 156 ***2.5. Fourier-Transform Infrared Spectroscopic (FT-IR) analysis***

157 The obtained three fractions (grape stalk powder as it is, acetylated and silylated  
158 powders) were subjected to the attenuated total reflectance Fourier-transform infrared  
159 spectroscopic analysis (ATR-FT-IR, Vertex 70, Bruker, Milan, Italy). The instrument  
160 was equipped with a Golden Gate™ (Specac) high-performance single reflection  
161 monolithic diamond sampling accessory, featuring a Type IIIA diamond ATR element  
162 metal-bonded into a tungsten carbide mount. Data were collected using OPUS software  
163 v6.5 (Bruker). For each sample, 32 spectra were obtained and co-added for each sample  
164 at a resolution of 4 cm<sup>-1</sup>. A background spectrum was obtained by collecting 32 co-  
165 added scans after the crystal was cleaned with acetone.

166

## 167 ***2.6. Bulk density and particle density***

168 The bulk density (including the contribution of the inter particulate void volume) of the  
169 samples was measured with the 10 mL graduated cylinder, while the particle density (or  
170 true density, that is the mass of a particle divided by its volume, excluding open and  
171 closed pores) was measured using a pycnometer AccuPyc 1330 (WHO, 2012).

172

## 173 ***2.7. Procedure for the production of bio-composite materials***

174 Firstly, 150 g of PBS and 1.5 g of paraffin oil were manually mixed to make the  
175 polymer wet and sticky, thus improving the adhesion between grape stalks and pellets  
176 surface as well as the polymer-filler homogeneity before extrusion. Subsequently, 15 g  
177 of grape-stalk fractions were added to the polymer (concentration of 10 parts for  
178 hundred parts of rubber, phr). Four different fractions were used: (i) grape stalk powder  
179 as it is (PBS 10GS), (ii) acetylated powder (PBS 10AcGS), and (iii) silylated powder  
180 (PBS 10SilGS). A variant of PBS 10SilGS was prepared by mixing in the extruder 1 phr

181 of silane with 150 g PBS and with 10 phr of untreated grape stalks powder in order to  
182 obtain (iv) a silanization *in situ* (PBS 10SilSituGS) sample. The different formulations  
183 were extruded with a twin-screw extruder (557 Rheomex, Haake S.r.l., Rezzato BS,  
184 Italy) using the following temperatures (feed zone, barrel, and die): 80, 120, and 125 °C  
185 and a screw speed of 50 rpm. The extruded materials were air-cooled, manually  
186 spooled, and then granulated. The four granulates were processed by injection molding  
187 machine (MegaTech TecnicaDueBi injection molding machine, Fabriano, Italy) in order  
188 to obtain specimens for the mechanical analysis of the bio-composite materials, for the  
189 color measurements, and for the morphological and infrared spectroscopic analysis  
190 (Seggiani et al., 2017). Injection molding was conducted using a temperature profile  
191 ranging from 90 °C (hopper zone) to 170 °C (die zone), a holding pressure of 40 bar, a  
192 holding time of 3 sec and a cooling step of 6 sec. As a comparative reference, PBS was  
193 also processed under the same conditions mentioned above (PBS proc).

194

## 195 **2.8. Scanning electron microscope - Field emission gun (SEM-FEG)**

196 A scanning electron microscope (Nova NanoSEM 450, SEM-FEG, FEI Europe B.V.,  
197 Hillsboro, USA), operating in low-vacuum conditions and equipped with a  
198 microanalysis X-EDS detector (QUANTAX-200, Bruker Corporation, Billerica, USA)  
199 was used to analyze the morphology of the PBS-based samples as well as of both  
200 untreated and treated grape stalks powders. In the case of PBS-based specimens, they  
201 were broken down into liquid nitrogen and the cross-section surface was observed,  
202 while in the case of grape stalks powder, they were directly observed after drying.

203

## 204 **2.9. Thermogravimetric analysis**

205 Thermogravimetric analysis (TGA) was carried out to evaluate the thermal stability of  
206 the grape stalks' powders and of the PBS-based composites. Tests were conducted on  
207  $15 \pm 2$  mg of each sample in a Perking-Elmer TGA 4000 instrument (Waltham, USA),  
208 using a temperature ramp of  $10 \text{ }^\circ\text{C min}^{-1}$  from  $40 \text{ }^\circ\text{C}$  to  $600 \text{ }^\circ\text{C}$  under inert atmosphere  
209 (nitrogen flow of  $40 \text{ mL min}^{-1}$ ).

210 The moisture uptake (MU) content was evaluated as the percentage decrease of the filler  
211 mass between  $40$  and  $100 \text{ }^\circ\text{C}$ .  $T_5$  and  $T_{15}$  were obtained from the thermograms as the  
212 temperatures at which the samples exhibited a mass loss of 5 and 15%wt., respectively,  
213 while  $R_{600}$  was obtained as the residual percentage mass of the sample evaluated at  
214  $600 \text{ }^\circ\text{C}$ . The degradative peak temperatures ( $T_{\text{peak}}$ ) were calculated as the temperatures  
215 at which the maximum derivative weight with respect to temperature (differential  
216 thermal analysis, DTA) occurred. In addition, the TGA data obtained from grape stalks  
217 powders and from PBS-based composites were fitted to the mathematical model  
218 proposed by Nabinejad et al. (2015) in order to determine the effective amount of GS  
219 filler ( $P_f$ ) present within PBS-based composites. The idea behind this model is that by  
220 increasing the filler loading, the thermogravimetric (TG) behavior of the composite  
221 material would become more and more similar to the behavior of the neat filler. The  
222 actual amount of filler within composites is very important since it provides indications  
223 on the processing capacity of the formulation and allows for a finer discussion of the  
224 composites' mechanical properties. In this context, the actual GS filler contents ( $P_f$ )  
225 obtained were used as an input for the micro-mechanical models described in the next  
226 section. The model proposed by Nabinejad et al. (2015) is based on the following  
227 formula:

$$228 \quad P_f(\%) = \alpha m_{dc} + \beta R_{600,c}(1)$$

229 where  $P_f$  represents the effective mass percentage of the filler within the composite,  $m_{dc}$   
230 is the percentage mass loss of composite evaluated at the  $T_{peak}$  of the filler, and  $R_{600,c}$  is  
231 the percentage mass residue of the composite at 600 °C. The mass drop coefficient  $\alpha$   
232 and the mass residue coefficient  $\beta$  can be calculated as follows:

$$233 \quad \alpha(-) = \frac{R_{600,p}}{R_{600,p}M_{df} - R_{600,f}M_{dp}} 100(2)$$

$$234 \quad \beta(-) = \frac{-M_{dp}}{R_{600,p}M_{df} - R_{600,f}M_{dp}} 100(3)$$

235 where  $R_{600,f}$  and  $R_{600,p}$  are the percentage mass residues evaluated at 600 °C of the neat  
236 filler and of the neat polymer, respectively, while  $M_{df}$  and  $M_{dp}$  are the percentage mass  
237 decreases of the neat filler and polymer evaluated at  $T_{peak,f}$ .

238

## 239 **2.10. Mechanical properties and micro-mechanical analysis**

240 Tensile tests were performed using a dynamometer (5567, Instron, Pianezza, Italy)  
241 equipped with a load cell of 1 kN and an extensometer of 25 mm. Tests were conducted  
242 with a 10 mm/min clamp separation speed. Young's modulus (E), tensile strength ( $\sigma_M$ ),  
243 and elongation at break ( $\epsilon_b$ ) values were reported as the average of ten measurements.  
244 The intrinsic stiffness of grape stalks fibers ( $E_P$ ) was obtained by applying two  
245 micromechanical models often used for the prediction of the Young's modulus of  
246 composites ( $E_C$ ), namely the Voigt model (1889) and the Halpin-Tsai model (Halpin,  
247 1969). The Voigt equation is generally used to predict the elastic modulus of composite  
248 materials where reinforcing fibers are supposed to be disposed in a parallel direction to  
249 the axial loading (Voigt, 1889) (parallel model). The Halpin-Tsai model is used to  
250 predict, in a simple and semi-empirical manner, the moduli of composites reinforced by  
251 short aligned fibers. In spite of the fact that these models do not account for many

252 factors such as the variability in the modulus of constituents and the effect of the  
253 compounding process (Battezzato et al., 2019), they have already been successfully  
254 applied to estimate the elastic modulus of several natural fillers/fibers (Ahankari et al.,  
255 2011).

256 Similarly, Pukanszky's equation (Pukanszky, 1990), which is generally used to predict  
257 the tensile strength of composite materials filled with short-fibers or quasi-spherical  
258 fillers, was applied to the tensile strength data of PBS-based samples to obtain the  
259 empirical adhesion B factor. The adhesion B factor is a useful tool to quantify and  
260 compare the effectiveness of the particle-matrix adhesion in different composites. The  
261 mentioned equations are reported as follows:

262 *Voigt*:  $E_C = E_P V_P + E_M (1 - V_P)$  (4)

263 *Halpin - Tsai*:  $E_C = E_M \frac{1 + 2\eta V_P}{1 - \eta V_P}$  with  $\eta = \frac{\frac{E_P}{E_M} - 1}{\frac{E_P}{E_M} + 2}$  (5)

264 *Pukanszky*:  $\sigma_C = \sigma_M \frac{1 - V_P}{1 + 2.5V_P} \exp(BV_P)$  (6)

265

266 where  $E_C$  is the composite modulus,  $E_M$  is the polymer matrix modulus,  $E_P$  is the filler  
267 particle modulus,  $V_P$  is the filler particle volume fraction,  $\sigma_C$  is the composite tensile  
268 strength,  $\sigma_M$  is the polymer matrix tensile strength and B is the Pukanszky's empirical  
269 adhesion constant.

270 TA DMA Q800 instrument was used in the single cantilever flexural configuration to  
271 evaluate the dynamic mechanical behavior of the different PBS-based samples  
272 exploiting rectangular specimens with the following sizes (l, w, t);  $17 \times 5 \times 2 \text{ mm}^3$ .

273 DMA tests were run with a heating rate of 3 °C/min from -40 to 100 °C with the  
274 oscillation frequency and the strain set at 1 Hz and 0.1%, respectively.  
275 For each sample, the storage modulus ( $E'$ ) and the  $\tan \delta$  (damping factor) (Saba et al.,  
276 2016) were plotted as temperature's functions while the glass transition temperature  
277 ( $T_g$ ) was evaluated as the temperature at which the maximum  $\tan \delta$  value was observed.

278

### 279 ***2.11. Thermal properties***

280 The thermal properties of the PBS-based samples were evaluated by Differential  
281 Scanning Calorimetry (DSC) (DSC TA 2010). DSC measurements were performed  
282 using  $10 \pm 2$  mg of sample and 50 mL/min of nitrogen as purging gas. Each sample was  
283 first heated up to 200 °C at 15 °C/min in order to erase the previous thermal history.  
284 Subsequently, samples were cooled to 0 °C at 10 °C/min and re-heated to 200 °C at  
285 10 °C/min. Crystallization temperature ( $T_C$ ) and crystallization enthalpy ( $H_C$ ) were  
286 evaluated during the cooling cycle meanwhile melting temperature ( $T_m$ ) and melting  
287 enthalpy ( $H_m$ ) were assessed from the second heating cycle. The crystallinity percentage  
288 ( $\chi$ ) was determined considering the weight fraction occupied by the additives and the  
289 value of 110 J/g as a reference for the 100% crystalline PBS melting enthalpy (Xu and  
290 Guo, 2010).

291

### 292 ***2.12. Color measurements***

293 CIELab coordinates ( $L^*$ ,  $a^*$ ,  $b^*$ ) were measured on the functionalized powder samples  
294 and specimens through a tristimulus colorimeter (Chroma Meter CR-400, Konica  
295 Minolta, Milan, Italy) in transmittance mode over the visible spectrum (from 380 to 770  
296 nm), using the illuminate D65 and 10° standard observer (McLaren, 1976). Chroma (C),

297 hue (H), and color distance (CD) were calculated according to the formula described by  
298 Hunt and Pointer (2011).

299

### 300 ***2.13. Statistical analysis.***

301 Univariate analyses were carried out on the data set. Differences among varieties were  
302 assessed by analysis of variance (one-way ANOVA) based on three replicates for each  
303 sample. When a significant effect (at least  $p \leq 0.05$ ) was shown, comparative analyses  
304 were carried out by the post hoc Tukey's multiple comparison test. All tests were  
305 performed with Statistica v8.0 software (Stat Soft Inc., Tulsa, USA).

306

## 307 **3. Results and discussion**

### 308 ***3.1. Yields and physical characterization of the functionalized grape stalk powders***

309 Grape stalks are lignocellulosic materials with a reported composition of cellulose (20-  
310 30%), hemicellulose (15-25%), lignin (20-30%), tannins (around 16%) and ashes (4-6%)  
311 (Prozil et al., 2012, Prozil et al., 2014, Spigno et al., 2013). All these compounds are  
312 characterized by the strong presence of hydroxyl groups, which well-lend themselves to  
313 chemical derivatization reactions used to obtain more lipophilic lignocellulose structures  
314 which, in turn, display an improved interaction with PBS polymer chains.

315 The grape stalk powder as it is and those functionalized were tested as fillers for the  
316 realization of bio-composite materials with polybutylene succinate. The powder  
317 subjected to acetylation reaction gave a yield of 31.19 g (62%) starting from 50.00 g of  
318 raw material, while the one treated by silanization yielded 24.34 g starting from 25.00 g  
319 of initial material.

320 The bulk density and particle density (or true density) measurements are shown in Table  
321 1. The functionalized samples showed significantly lower density values ( $p \leq 0.01$ ) as  
322 compared to the untreated powder, thus confirming their decrease as the subsequent  
323 effect of the derivatization reaction. This can be explained by the breakdown of the  
324 intra- and intermolecular hydrogen bonds, which are usually responsible for the native  
325 configurations of cellulose and hemicellulose macromolecules (Jarvis, 2018).

326 The structural analysis of the derivatized grape stalk powder was carried out with FT-IR  
327 spectroscopy to highlight different functional groups between the control sample and  
328 the modified ones. Fig. 1a shows the infrared spectra of the control sample as it is, the  
329 acetylated and the silylated powders. In the FT-IR spectrum of the control sample, the  
330 band relating to the stretching of the hydroxyl group ( $3330 \text{ cm}^{-1}$ ) appeared to be  
331 relevant, while in the spectrum of the corresponding material functionalized through  
332 acetylation this band was almost absent. Conversely, the band relating to the stretching  
333 of the carbonyl group ( $1720 \text{ cm}^{-1}$ ) showed a significant increase as a consequence of the  
334 acetylation reaction. Similar considerations cannot be done for silylated powder,  
335 probably due to the poor reactivity of the silylating reagent towards the grape stalk  
336 powder.

337 From a morphological point of view, the SEM images of the surface of both untreated  
338 and treated grape stalk powders were reported in Fig. 1b, 1c, and 1d. Looking at the  
339 untreated grape stalk powder (Fig. 1b), many surface impurities can be observed,  
340 especially close to the edges of the GS particles and fibers. On the contrary, Fig. 1c  
341 shows that acetylation reaction removed nearly all the impurities from the particle and  
342 fiber surface. Indeed, during acetylation, waxy substances of fibers/particles are  
343 dissolved and hydroxy groups are replaced by acetyl groups, as other similar works also

344 reported (Le Troedec et al., 2008, Pickering et al., 2007, Tserki et al., 2005). In addition,  
345 SEM micrographs also show that the surfaces of the acetylated grape stalks were  
346 rougher and spongier than those of the untreated grape stalks. This behavior, which can  
347 be explained by the esterification reactions leading to higher surface roughness and  
348 porosity (Li et al., 2007), is a positive feature since rougher surfaces have higher  
349 chances of mechanically interlocking with polymer chains during melt compounding  
350 (Hajiha et al., 2014). The SEM images of grape stalks before and after silane treatment  
351 (Fig. 1b and 1d, respectively) are not significantly different in terms of morphology.  
352 Similar results were also reported by other studies on silanization of fibers, where the  
353 surface morphology was not found to have been modified by the -OH group silanization  
354 (Sawpan et al., 2011, Suardana et al., 2011). Nevertheless, it can be noticed that  
355 silylated grape stalks have fewer impurities on their surface compared to untreated  
356 grape stalks. It is noteworthy to notice that elemental analysis of silylated grape stalks  
357 obtained through X-EDS (Fig. S2c) showed the presence of silicon (around 1%wt.) in  
358 the fibers/particles, which proves its successful reaction.

359 Finally, the TGA data (under nitrogen atmosphere) of untreated and treated grape stalks  
360 are shown in Table 1 and in Fig. S3. It can be noticed that GS and SilGS exhibited a  
361 similar behavior in terms of thermal stability. Both samples exhibited two peaks of  
362 degradation (peak 1 and peak 2 of the DTA curves); the first one occurred at around  
363 193 °C, while the second one at 309 °C. From a qualitative point of view, the first  
364 degradative peak can be associated to the loss of the hemicellulose fraction, which is  
365 less stable than cellulose and lignin (the latter being the most stable of the two)  
366 (Ramiah, 1970), while the second degradative peak can be attributed to the loss of  
367 cellulose. Conversely, AcGS (Fig. S3b) only showed a single marked mass loss step at

368 around 344 °C, while peak 1 was almost absent. It is reasonable to suppose that AcGS  
369 exhibited only a slight first degradative peak because the hemicellulose fraction could  
370 have been depolymerized under the strong conditions of acetylation reaction (Zhao et  
371 al., 2020). This hypothesis has been partially confirmed by the FT-IR spectra reported in  
372 Fig. 1a where the –OH peak of AcGS is much less marked than in GS and SilGS. As a  
373 consequence, AcGS seems to be the most stable powder, a finding which has also been  
374 confirmed by the T<sub>15</sub> value (the temperature at which 15% of mass loss is observed)  
375 which was roughly 30 °C higher than the values found in GS and SilGS.  
376 From an application point of view, the T<sub>15</sub> of each tested powder was much higher than  
377 the PBS processing temperatures, thus confirming the possibility of exploiting grape  
378 stalks as natural fillers within PBS. Looking at the final part of the TG curves, GS and  
379 SilGS exhibited residues values (R<sub>600</sub>) almost two times higher than AcGS. Again, this  
380 result can be explained by the fact that the hemicellulose was partially removed during  
381 the acetylation reaction. Finally, a reduction from 38% (SilGS) to 48% (AcGS) in  
382 moisture uptake was found in treated grape stalks, thus confirming the hydrophilicity  
383 reduction in grape stalks following surface treatments. This aspect is particularly  
384 important from an application point of view since fillers need to be dried before they  
385 can compound with bio-polyesters in order to avoid possible degradative hydrolysis  
386 reactions of the polymer chains.

387

### 388 ***3.2. Thermal properties of the bio-composites***

389 The thermal properties (T<sub>g</sub>, T<sub>c</sub>, T<sub>m</sub>, and  $\chi$ ) of the PBS-based samples, evaluated by  
390 Differential scanning calorimetry (DSC), are reported in Table 2. No significant  
391 differences in the thermal behavior of PBS were showed by adding grape stalks as

392 fillers. Moreover, also the typology of the surface treatment did not exhibit any  
393 particular behavior. Considering the melting and crystallization temperatures ( $T_m$  and  
394  $T_c$ ), the maximum deviations were observed in the PBS 10SiIGS sample, in which  $T_m$   
395 and  $T_c$  were lower than 0.6 and 1.5 °C, respectively, if compared with pure PBS.  
396 Similarly, the PBS crystallinity appeared unchanged by the addition of grape stalks. In  
397 general, when their particle size is markedly low, natural fillers can act as nucleating  
398 agents, thus accelerating and increasing the formation of crystalline domains (Kai et al.,  
399 2005, Väisänen et al., 2017, Zhang et al., 2012). In the present case, the unchanged  
400 crystallinity pointed out the necessity to further optimize the grinding step in order to  
401 enhance the crystal domain. Nevertheless, the grape stalk particles were not too coarse,  
402 as testified by the fact that crystallinity was not decreased. Indeed, when using too gross  
403 fillers, the agglomeration phenomena can inhibit the crystallization (Nanni and Messori,  
404 2020a).

405 In order to evaluate the thermal stability of the PBS-based composites,  
406 thermogravimetric analysis (TGA) was conducted by heating samples taken from the  
407 tensile specimens from a starting temperature of 40 °C up to 600 °C under inert  
408 atmosphere (nitrogen). The obtained TG and DT curves and data are reported in Fig. 2  
409 and in Table 2, respectively. Neat PBS degraded in one fast mass loss step between 300  
410 and 400 °C, as other authors have also reported (Chrissafis et al., 2005, Nanni et al.,  
411 2020). Looking at Fig. 2a, it is evident that the same degradative behavior was also  
412 observed in PBS samples filled with grape stalks. Nevertheless, in composites, the TG  
413 curves had shifted to the left (lower temperatures) of about 20-30 °C. In particular, the  
414  $T_5$  temperatures (temperatures at which 5% of mass loss is reached) of PBS-based  
415 composites were particularly lower compared to the temperature of neat PBS (around -

416 44 °C in the case of GS and SilGS) and this fact can be explained by the intrinsic lower  
417 thermal stability of the hemicellulose fraction present within grape stalks. These earlier  
418 mass losses do not represent an application problem since the  $T_5$  temperatures were  
419 much higher than the processing conditions of PBS polymer. Moreover, looking at the  
420 values of  $T_{15}$ , which is generally used as reference for the maximum temperature  
421 applicable to a polymer, no differences among filled and neat PBS are evident. From a  
422 comparative point of view, PBS 10AcGS sample exhibited the higher  $T_5$  value, which is  
423 in perfect agreement with the intrinsic higher thermal stability of the acetylated grape  
424 stalks (Table 1). Finally, TG data were also fitted with equations 1-3 to evaluate the  
425 actual content of the filler within the composite ( $P_f$ ). As reported in Table 2, the  
426 mathematical model reported an actual amount of filler consistent with the processed  
427 formulation for all samples except for PBS 10SilSitu. In this case, the model showed  
428 that only 6.2%wt. of grape stalks were present within the PBS matrix. This data is  
429 reasonably correct because, as further shown, both the TG and the mechanical data of  
430 PBS 10SilSitu are midway in between the ones of neat PBS and 10%wt. filled  
431 composites, thus implying it has a mid-term content of filler. It is fair to suppose that,  
432 during reactive extrusion, grape stalks, with the aid of sticky silane, formed aggregates  
433 which were not transported by the screws of the extruder; further work should verify  
434 this hypothesis.

435 The actual filler content resulting from the model was used as an input to obtain other  
436 micro-mechanical parameters, as the section 3.3 shows. All parameters of equations 1-3  
437 are available in the supplementary data file.

438

### 439 ***3.3. Tensile properties of the bio-composites***

440 In Table 2 and in Fig. S4, the tensile properties of the bio-composites are reported. In  
441 each case, the grape stalks enhanced the pure PBS Young's modulus of around 17-18%.  
442 Such an increase in stiffness could be linked to the hydrophobic interactions as well as  
443 to the hydrogen-bonds electrostatic forces occurring between the modified  
444 lignocellulosic material and the co-polymer (Bharath and Basavarajappa, 2016, Mu et  
445 al., 2018). The functionalization of lignocellulosic fiber led to an increase in the contact  
446 interfaces between the copolymer and the lignocellulosic filler (Borsoi et al., 2019,  
447 Gwon et al., 2010b).

448 Nevertheless, Young's modulus is only moderately affected by the particle-polymer  
449 adhesion since this property is evaluated at low deformations in which separation  
450 phenomena of particle-matrix interface generally do not occur (Fu et al., 2008, Nanni  
451 and Messori, 2020a). This hypothesis is also supported by the fact that even PBS 10GS  
452 (untreated grape stalks) showed an increased elastic modulus value. Therefore, the  
453 increase in Young's modulus is mainly explained by the fact that GS particles are  
454 intrinsically stiffer and harder than the PBS matrix. The stiffness of lignocellulosic  
455 materials such as grape stalks generally depends on the amounts of cellulose,  
456 hemicellulose and lignin they contain, since cellulose (140 GPa) is much stiffer than  
457 hemicellulose (8 GPa) while lignin normally acts as a coupling bonding agent (between  
458 cellulose and hemicellulose) rather than as stiffening element (Cousins, 1978,  
459 Gurunathan et al., 2015). Therefore, the high content of cellulose (20-30%wt.) within  
460 grape stalks could explain the gain in elastic modulus observed in the PBS-based  
461 composites. In addition, the fact that PBS 10AcGS exhibited the highest Young's  
462 modulus could be due to the degradation of hemicellulose during the acetylation  
463 reaction.

464 The GS elastic moduli ( $E_P$ ), obtained by applying the theoretical models of Voigt and  
465 Halpin-Tsai on the experimental data, are reported in Table 3. These models require as  
466 input the filler volume of fractions ( $V_P$ ), which were calculated using the actual filler  
467 contents ( $P_f$  values in Table 3) and the particle densities (Table 1). The Voigt model  
468 gave  $E_P$  values lower than the ones obtained using the Halpin-Tsai model although its  
469 standard deviation was lower than the one observed in the Halpin-Tsai model.  
470 Nevertheless, both models provided comparable  $E_P$  values and thus it can be estimated  
471 that the intrinsic grape stalks Young's modulus ranges between 1.3 and 1.8 GPa. It is  
472 interesting to notice that GS stiffness was lower but similar to the one reported for lees  
473 filtered from the wine mass (between 1.8 and 2.5 GPa), that were tested with PBS at 10  
474 phr loading (Nanni and Messori, 2020b).

475 In the case of PBS 10SilSituGS, if a filler content input of 10%wt. ( $V_P$  of 0.12) was  
476 used, the Voigt and Halpin-Tsai models would have given  $E_P$  values of 1096 and 1239  
477 MPa, respectively, which are considerably lower compared to the other ones. Actually,  
478 using the 6.2%wt. value, the obtained  $E_P$  values (Table 3) are more consistent with the  
479 others, thus pointing out the reliability of the equations 1-3 previously fitted on TGA  
480 data.

481 Looking at the tensile strength data ( $\sigma_M$ ) reported in Table 2, the presence of grape  
482 stalks lowers this mechanical property of around 10-20%, compared with neat PBS.  
483 However, this loss was not so dramatic if compared to other studies in which PBS bio-  
484 composites showed tensile strength values 26-31% lower than pure PBS (Sahoo et al.,  
485 2011, Then et al., 2013). This aspect can be explained by a good adhesion between the  
486 PBS matrix and the GS particles. Indeed, in polymer composites, the tensile strength  
487 mainly depends on the particle-matrix adhesion since well-bonded particles can better

488 transfer the stress load across the interface while poor adhesion leads to physical  
489 discontinuities unable to support mechanical loads. (Borsoi et al., 2019, Fu et al., 2008).  
490 FT-IR analysis on the biocomposites was performed, however, there were no  
491 differences in the FT-IR spectra of the various samples, and for this reason the spectra  
492 were not shown. As a matter of fact, the carbonyl band of PBS far outweighs the added  
493 one thanks to the contribution given by the acetylated grape stalks.  
494 In Fig. 3, SEM-FEG images of PBS 10GS and PBS 10AcGS surfaces were reported in  
495 order to make a qualitative investigation of the interactions between grape stalks fillers  
496 and PBS matrix. From micrographs taken at lower magnifications (Fig. 3a and 3b), it  
497 can be noticed that grape stalks fillers were homogeneously distributed and well  
498 dispersed through the surface of both composites. By increasing the magnification (Fig.  
499 3c and 3d), it is possible to notice that acetylated grape stalks were well connected with  
500 the PBS matrix and that adhesion problems were not detectable. This positive behavior,  
501 indirectly proved by the high tensile strength values, is the consequence of both  
502 chemical and physical aspects. Indeed, acetylation lowered the grape stalks polarity,  
503 thus improving the chemical bond between PBS and GS and it also enhanced the grape  
504 stalk roughness, thus promoting physical interconnections between polymer and fillers.  
505 In addition, untreated grape stalks overall exhibited a good adhesion within PBS,  
506 though in this case, cap-shaped cavities caused by particles which had not bonded well,  
507 were also detected.  
508 In order to quantify the adhesion, the empirical B adhesion factor was extrapolated by  
509 applying Pukanzky's equation on the experimental data. This factor increases in parallel  
510 with the increase of the particle-matrix adhesion and approaches zero for scarcely  
511 compatible particles. The untreated GS continued to show positive B values (0.99) and

512 the surface treatments enhanced the particle-matrix adhesion (Table 3). In particular,  
513 PBS 10AcGS showed the highest B value (2.07), thus highlighting the efficiency of the  
514 acetylation treatment.

515 PBS 10SilSituGS showed the highest tensile strength ( $\sigma_M$ ) value among the other filled  
516 composites, but, again, this result is mainly due to the lower actual content of filler  
517 within the PBS matrix. Indeed, composites' tensile strength generally decreases by  
518 increasing the filler loading and *vice versa* (Fu et al., 2008). Therefore, to compare the  
519 adhesion effectiveness of this formulation it is useful to refer, once more, to the  
520 Pukanszky's B empirical factor. In the case of PBS 10SilSituGS, the B value is 1.52  
521 which is higher than PBS 10GS (0.99) but lower than PBS samples filled with treated  
522 grape stalks. In other words, the grafting reaction of silane in reactive extrusion  
523 improved the filler-matrix adhesion but did not do so as effectively as the direct  
524 functionalization of the grape stalks.

525

### 526 ***3.4. Dynamic mechanical analysis***

527 In order to thoroughly evaluate the reinforcement effect of GS, dynamic mechanical  
528 analysis (DMA) was also performed. The results were consistent with the tensile  
529 properties. In Fig. 4a the storage modulus ( $E'$ ) of each PBS-based sample is reported as  
530 a function of the temperature ranging from 0 °C to 100 °C. Filled samples showed  
531 enhanced  $E'$  values, especially in the range 0-50 °C, while in the range 50-100 °C the  
532 gap seemed to decrease, especially when comparing PBS 10GS and PBS proc.  
533 Nevertheless, it is noteworthy to underline that PBS 10AcGS and silylated stalks  
534 guarantee  $E'$  increments of nearly 15% even at temperatures ranging from 80 to as high  
535 as 100 °C.

536 Fig. 4b shows the diagram of the relationship between  $\tan \delta$  and temperature in a range  
537 of -40 to 0 °C. The glass transition temperature ( $T_g$ ), defined as the temperature at  
538 which the maximum  $\tan \delta$  value is observed, was only slightly enhanced by the GS  
539 fillers, shifting approximately from -20 to -19 °C. This information, combined with the  
540 fact that also the highest  $\tan \delta$  value showed only a moderate increase proves an  
541 effective interfacial adhesion that reduced the PBS chain mobility (Leszczyńska et al.,  
542 2018).

543 Nevertheless, it could be suggested that the volume of the constrained chains was not  
544 too significant. This hypothesis is indeed supported by the thermal properties, reported  
545 in Table 1, where no significant variations in the melting temperature ( $T_m$ ) and in the  
546 crystallinity percentage ( $\chi$ ) were observed. In fact, in the case of important flexibility  
547 reductions,  $T_m$  of filled samples would have been higher than the one observed in pure  
548 PBS and  $c$  would have been lower (Giubilini et al., 2020).

549

### 550 **3.5. Color Measurements**

551 The visual analysis of the specimens highlighted a clear chromatic difference with the  
552 naked eye (Fig. 5a). The results of the colorimetric evaluation using the CIELab ( $L^*$ ,  $a^*$ ,  
553  $b^*$ ) color space are shown in Table S3. The most interesting results were the remarkably  
554 lower ( $p \leq 0.001$ )  $L^*$ ,  $a^*$ , and  $b^*$  values shown by the acetylated samples (powder and  
555 specimens) in comparison with the ones related to the controls and silylated samples.  
556 This further confirms the strong alteration that occurred during the acetylation reaction  
557 in comparison with the silylated one. In the CIELab color space,  $L^*$  is used to indicate  
558 the brightness, while the positive-negative  $a^*$  is the redness-greenness index and the  
559 positive-negative  $b^*$  the yellowness-blueness one.

560 The colorimetric evaluation was also carried out considering the determination of the  
561 color indices chroma and hue (Table S3). The chroma corresponds to the colorfulness of  
562 an area judged in proportion to the brightness and this color index was higher for the  
563 powder as it is and for the silylated sample as compared to the acetylated sample.  
564 Similarly, the bio-composites obtained from the powders as they are and from the  
565 silylated ones had higher chroma values than those deriving from acetylated samples.  
566 The hue is the attribute of a visual perception according to which an area appears to be  
567 similar to one, or to proportions of two, of the perceived colors, red, yellow, green, and  
568 blue. In the powders and in the biocomposite specimens this index was lower for  
569 acetylated samples than for the control and the silylated ones. For this reason, the color  
570 distances showed higher values when comparing the acetylated powders and specimens  
571 with the corresponding remainder (Fig. 5b and 5c). When the color distance exceeds the  
572 threshold value of 5, the human eye is capable of perceiving a color difference between  
573 two objects (Musetti et al., 2015).  
574 The differences in the values of chroma and hue were due to the fact that in the  
575 acetylation reaction there was an increase in the carbon content, which caused a  
576 decrease in brightness and hue (Cai et al., 2019). In fact, carbon was also added with  
577 silanization and the reduced color distance when compared to the controls could be  
578 further confirmation of the partial functionalization.

579

#### 580 **4. Conclusions**

581 In this work, the possible valorization of grape stalks' by-products as newly-evaluated,  
582 cost-advantageous and natural reinforcing fillers within poly(butylene succinate) (PBS)  
583 was ascertained. Among all tested grape stalks-derived fillers, acetylated grape stalks

584 (AcGS) showed the best mechanical performance. Indeed, as confirmed by FT-IR and  
585 SEM-FEG analyses, the acetylation reaction rendered the surface of grape stalks more  
586 hydrophobic, as well as rougher and spongier. The combination of these chemical and  
587 physical modifications resulted in a good particle-polymer matrix adhesion which led to  
588 satisfactory mechanical properties.

589 Aside from the improved mechanical properties, the incorporation of 10-phr grape stalk  
590 powder into a biodegradable polymer as polybutylene succinate leads to reduced use of  
591 the polymer and thus lowers the cost of the finished material besides providing several  
592 different woody hues. It also permits the valorization of by-products derived from the  
593 wine industry such as grape stalks which are usually accumulated in huge quantities and  
594 also represent a high cost in terms of disposal. This project could, therefore, have a  
595 strong impact on the circular economy in pushing it to study and make use of  
596 biomaterials derived from food waste.

597

## 598 **Acknowledgments**

599 This work was supported by the Emilia-Romagna Region, Italy, [grant number CUP  
600 E81I18003220009 *Bando Alte Competenze*, “Recovery of useful molecules from low-  
601 value waste of the wine industry” (Ref. PA: 2016-8349/RER), PO FSE 2014-2020  
602 “Safety, Quality and Integration of regional agri-food chains to increase their  
603 competitiveness”].

604 The authors wish to thank Dr. Sara Ronconi (English-language reviewer) for her  
605 valuable contribution to the drafting of the present article. Moreover, we thank the Bank  
606 Foundation “Cassa di Risparmio di Modena” for the FT-IR and SEM-FEG instruments  
607 used in the CIGS Interdepartmental Centre of the University of Modena and Reggio

608 Emilia, as well as Dr Fabio Bergamini and Dr Massimo Tonelli for their advice and  
609 valuable support. We thank the C.R.P.A. lab (Technopole of Reggio Emilia) for the use  
610 of the Pulverisette 19 mill.

611

#### 612 **Conflict of Interest Statement**

613 The authors declare that there is no conflict of interest regarding the publication of this  
614 article.

615

#### 616 **Data Availability statement**

617 The raw/processed data required to reproduce these findings cannot be shared at this  
618 time as the data is also part of an ongoing study.

619

## 620 References

- 621 Abdellaoui, H., Bouhfid, R., Qaiss, A.E.K., 2018. Lignocellulosic fibres reinforced thermoset composites:  
622 preparation, characterization, mechanical and rheological properties, in: S. Kalia (Ed.), *Lignocellulosic*  
623 *Composite Materials*, Springer, Cham, Switzerland, pp. 215–270. [https://doi.org/10.1007/978-3-319-](https://doi.org/10.1007/978-3-319-68696-7_5)  
624 [68696-7\\_5](https://doi.org/10.1007/978-3-319-68696-7_5)
- 625 Ahankari, S.S., Mohanty, A.K., Misra, M., 2011. Mechanical behaviour of agro-residue reinforced poly  
626 (3-hydroxybutyrate-co-3-hydroxyvalerate),(PHBV) green composites: A comparison with traditional  
627 polypropylene composites. *Compos. Sci. Technol.* 71(5) 653–657.  
628 <https://doi.org/10.1016/j.compscitech.2011.01.007>
- 629 Barba, F.J., Zhu, Z., Koubaa, M., Sant'Ana, A.S., Orlie, V., 2016. Green alternative methods for the  
630 extraction of antioxidant bioactive compounds from winery wastes and by-products: A review. *Trends*  
631 *Food Sci. Technol.* 49, 96–109. <https://doi.org/10.1016/j.tifs.2016.01.006>
- 632 Battezzatore, D., Noori, A., Frache, A., 2019. Natural wastes as particle filler for poly (lactic acid)-based  
633 composites. *J. Compos. Mater.* 53(6) 783–797. <https://doi.org/10.1177/0021998318791316>
- 634 Bevilacqua, N., Morassut, M., Serra, M.C., Cecchini, F., 2017. Determinazione dell'impronta carbonica  
635 dei sottoprodotti della vinificazione e loro valenza biologica. *Ingegneria dell'Ambiente* 4(3), 277–285.  
636 <http://dx.doi.org/10.14672/ida.v4i3.1142>
- 637 Bharath, K.N., Basavarajappa, S., 2016. Applications of biocomposite materials based on natural fibers  
638 from renewable resources: a review. *Sci. Eng. Compos. Mater.* 23(2), 123–133.  
639 <https://doi.org/10.1515/secm-2014-0088>
- 640 Borsoi, C., Menin, C., Lavoratti, A., Zattera, A.J., 2019. Grape stalk fibers as reinforcing filler for polymer  
641 composites with a polystyrene matrix. *J. Appl. Polym. Sci.* 136(18), 47427.  
642 <https://doi.org/10.1002/app.47427>
- 643 Brandt, A., Gräsvik, J., Hallett, J.P., Welton, T., 2013. Deconstruction of lignocellulosic biomass with  
644 ionic liquids. *Green Chem.* 15(3), 550–583. <https://doi.org/10.1039/C2GC36364J>
- 645 Brostow, W., Datashvili, T., Jiang, P., Miller, H., 2016. Recycled HDPE reinforced with sol–gel silica  
646 modified wood sawdust. *Eur. Polym. J.* 76, 28–39. <https://doi.org/10.1016/j.eurpolymj.2016.01.015>
- 647 Cai, S., Zhang, N., Li, K., Li, Y., Wang, X., Nantong, P.R., 2019. Effect of pressurized hot water  
648 treatment on the mechanical properties, surface color, chemical composition and crystallinity of pine  
649 wood. *Wood Research* 64(3), 389–400. <http://www.woodresearch.sk/wr/201903/02.pdf> (accessed 19  
650 January 2021).
- 651 Cancelli, U., Montevicchi, G., Masino, F., Mayer-Laigle, C., Rouau, X., Antonelli, A., 2020. Grape stalk:  
652 a first attempt to disentangle its fibres via electrostatic separation. *Food Bioprod. Process.* 124, 455–468.  
653 <https://doi.org/10.1016/j.fbp.2020.10.006>
- 654 Chrissafis, K., Paraskevopoulos, K., Bikiaris, D., 2005. Thermal degradation mechanism of poly  
655 (ethylene succinate) and poly (butylene succinate): comparative study. *Thermochim. Acta* 435(2), 142–  
656 150. <https://doi.org/10.1016/j.tca.2005.05.011>
- 657 Cousins, W., 1978. Young's modulus of hemicellulose as related to moisture content. *Wood Sci. Technol.*  
658 12(3), 161–167. <https://doi.org/10.1007/BF00372862>
- 659 Espert, A., Camacho, W., Karlson, S., 2003. Thermal and thermomechanical properties of biocomposites  
660 made from modified recycled cellulose and recycled polypropylene. *J. Appl. Polym. Sci.* 89(9), 2353–  
661 2360. <https://doi.org/10.1002/app.12091>

- 662 Fortea-Verdejo, M., Bumbaris, E., Burgstaller, C., Bismarck, A., Lee, K.Y., 2017. Plant fibre-reinforced  
663 polymers: where do we stand in terms of tensile properties? *Int. Mater. Rev.* 62(8), 441–464.  
664 <https://doi.org/10.1080/09506608.2016.1271089>
- 665 Fu, S.Y., Feng, X.Q., Lauke, B., Mai, Y.W., 2008. Effects of particle size, particle/matrix interface  
666 adhesion and particle loading on mechanical properties of particulate–polymer composites. *Composites*  
667 *Part B* 39(6), 933–961. <https://doi.org/10.1016/j.compositesb.2008.01.002>
- 668 Ghaffar, S.H., Fan, M., McVicar, B., 2015. Bioengineering for utilisation and bioconversion of straw  
669 biomass into bio-products. *Ind. Crops Prod.* 77, 262–274. <https://doi.org/10.1016/j.indcrop.2015.08.060>
- 670 Giubilini, A., Sciancalepore, C., Messori, M., Bondioli, F., 2020. New biocomposite obtained using  
671 poly(3-hydroxybutyrate-co-3-hydroxyhexanoate) (PHBH) and microfibrillated cellulose. *J. Appl. Polym.*  
672 *Sci.* 137(32), 48953. <https://doi.org/10.1002/app.48953>.
- 673 Gurunathan, T., Mohanty, S., Nayak, S.K., 2015. A review of the recent developments in biocomposites  
674 based on natural fibres and their application perspectives. *Compos. Part A Appl. Sci. Manuf.* 77, 1–25.  
675 <https://doi.org/10.1016/j.compositesa.2015.06.007>
- 676 Gustavsson, J., Cederberg, C., Sonesson, U., Van Otterdijk, R., Meybeck, A., 2011. Global Food Losses  
677 and Food Waste. FAO, Rome, pp. 1–38.
- 678 Gwon, J.G., Lee, S.Y., Doh, G.H., Kim, J.H., 2010a. Characterization of chemically modified wood fibers  
679 using FTIR spectroscopy for biocomposites. *J. Appl. Polym. Sci.* 116(6), 3212–3219.  
680 <https://doi.org/10.1002/app.31746>
- 681 Gwon, J.G., Lee, S.Y., Chun, S.J., Doh, G.H., Kim, J.H., 2010b. Effects of chemical treatments of hybrid  
682 fillers on the physical and thermal properties of wood plastic composites. *Composites Part A* 41(10),  
683 1491–1497. <https://doi.org/10.1016/j.compositesa.2010.06.011>
- 684 Hajiha, H., Sain, M., Mei, L.H., 2014. Modification and characterization of hemp and sisal fibers. *J. Nat.*  
685 *Fibers* 11(2), 144–168. <https://doi.org/10.1080/15440478.2013.861779>
- 686 Halpin, J.C., 1969. Stiffness and expansion estimates for oriented short fiber composites. *J. Composite*  
687 *Materials* 3(4), 732–734. <https://doi.org/10.1177/002199836900300419>
- 688 Hernandez Michelena, A., 2019. Natural fibre reinforced composite materials, PhD Thesis (University of  
689 Plymouth).
- 690 Hunt, R.W.G., Pointer, M.R., 2011. *Measuring Colour*, fourth ed. Wiley & Sons, New York (USA).
- 691 Hussain, M.A., 2004. Alternative routes of polysaccharide acylation: synthesis, structural analysis,  
692 properties, PhD Thesis (Friedrich-Schiller-Universität Jena).
- 693 Jarvis, M.C., 2018. Structure of native cellulose microfibrils, the starting point for nanocellulose  
694 manufacture. *Philos. Trans. R. Soc. London, Ser. A.* 376, 20170045.  
695 <https://doi.org/10.1098/rsta.2017.0045>
- 696 Kai, W., He, Y., Inoue, Y., 2005. Fast crystallization of poly(3-hydroxybutyrate) and poly(3-  
697 hydroxybutyrate-co-3-hydroxyvalerate) with talc and boron nitride as nucleating agents. *Polym. Int.*  
698 54(5), 780–789. <https://doi.org/10.1002/pi.1758>
- 699 Kalia, S., Thakur, K., Celli, A., Kiechel, M.A., Schauer, C.L., 2013. Surface modification of plant fibers  
700 using environment friendly methods for their application in polymer composites, textile industry and  
701 antimicrobial activities: A review. *J. Environ. Chem. Eng.* 1(3), 97–112.  
702 <https://doi.org/10.1016/j.jece.2013.10.011>
- 703 Leszczyńska, A., Stafin, K., Pagacz, J., Mičušík, M., Omastova, M., Hebda, E., Pielichowski, J.,  
704 Borschneck, D., Rose, J., Pielichowski, K., 2018. The effect of surface modification of microfibrillated

705 cellulose (MFC) by acid chlorides on the structural and thermomechanical properties of biopolyamide  
706 4.10 nanocomposites. *Ind. Crops Prod.* 116, 97–108. <https://doi.org/10.1016/j.indcrop.2018.02.022>

707 Le Troedec, M., Sedan, D., Peyratout, C., Bonnet, J.P., Smith, A., Guinebretiere, R., Gloaguenc, V.,  
708 Krausz, P., 2008. Influence of various chemical treatments on the composition and structure of hemp  
709 fibres. *Compos. Part A Appl. Sci. Manuf.* 39(3), 514–522.  
710 <https://doi.org/10.1016/j.compositesa.2007.12.001>

711 Li, X., Tabil, L.G., Panigrahi, S., 2007. Chemical treatments of natural fiber for use in natural fiber-  
712 reinforced composites: a review. *J. Polym. Environ* 15(1), 25–33. 10.1007/s10924-006-0042-3

713 Lieder, M., Rashid, A., 2016. Towards circular economy implementation: a comprehensive review in  
714 context of manufacturing industry. *J. Clean. Prod.*, 115, 36–51.  
715 <https://doi.org/10.1016/j.jclepro.2015.12.042>

716 Lucarini, M., Durazzo, A. Romani, A., Campo, M., Lombardi-Boccia, G., Cecchini, F., 2018. Bio-based  
717 compounds from grape seeds: A biorefinery approach. *Molecules.* 23(8), 1888.  
718 doi:10.3390/molecules23081888

719 Luzi, F., Torre, L., Kenny, J.M., Puglia, D., 2019. Bio-and fossil-based polymeric blends and  
720 nanocomposites for packaging: Structure–property relationship. *Materials.* 12(3), 471.  
721 <https://doi.org/10.3390/ma12030471>

722 MacArthur, E., 2013. *Towards the Circular Economy: Opportunities for the Consumer Goods Sector*,  
723 Ellen MacArthur Foundation, Cowes, UK.

724 Maicas, S., Mateo, J.J., 2020. Sustainability of Wine Production. *Sustainability.* 12(2), 559.  
725 <https://doi.org/10.3390/su12020559>

726 Maina, S., Kachrimanidou, V., Koutinas, A., 2017. A roadmap towards a circular and sustainable  
727 bioeconomy through waste valorization. *Curr. Opin. Green Sustainable Chem.* 8, 18–23.  
728 <https://doi.org/10.1016/j.cogsc.2017.07.007>

729 Masino, F. Chinnici, F., Bendini, A., Montevecchi, G., Antonelli, A., 2008. A study on relationships  
730 among chemical, physical, and qualitative assessment in traditional balsamic vinegar. *Food Chem.*  
731 106(1), 90–95. <https://doi.org/10.1016/j.foodchem.2007.05.069>

732 McLaren, K., 1976. XIII—The development of the CIE 1976 (L\* a\* b\*) uniform colour space and  
733 colour-difference formula. *J. Soc. Dyers Colourists* 92(9), 338–341. <https://doi.org/10.1111/j.1478-4408.1976.tb03301.x>

735 Mohammed-Ziegler, I. Tánzos, I., Hórvölgyi, Z., Agoston, B., 2008. Water-repellent acylated and  
736 silylated wood samples and their surface analytical characterization. *Colloids Surf. A Physicochem. Eng.*  
737 *Asp.* 319(1-3), 204–212. <https://doi.org/10.1016/j.colsurfa.2007.06.063>

738 Montevecchi, G., Masino, F., Antonelli, A., 2011. Pyroglutamic acid development during grape must  
739 cooking. *Eur. Food Res. Technol.* 232(2), 375–379. <https://doi.org/10.1007/s00217-010-1383-7>

740 Montevecchi, G., Simone Vasile, G., Matrella, V., Masino, F., Imazio, S. A., Antonelli, A., Bignami, C.,  
741 2014. Study of anthocyanin profile for valorization of autochthonous grapevine (*Vitis vinifera* L.)  
742 cultivars of the Emilia Romagna region, in: Warner, L.M. (Ed.), *Handbook of Anthocyanins: Food*  
743 *Sources, Chemical Applications and Health Benefits.* Nova Science Publishers Inc., Hauppauge, USA,  
744 pp. 197–216.

745 Mu, B., Wang, H., Hao, X., Wang, Q., 2018. Morphology, mechanical properties and dimensional  
746 stability of biomass particles/high density polyethylene composites: Effect of species and composition.  
747 *Polymers.* 10(3), 308. <https://doi.org/10.3390/polym10030308>

748 Musetti, A., Tagliazucchi, D., Montevecchi, G., Verzelloni, E., Antonelli, A., Fava, P., 2015.  
749 Characterization of a combined treatment with alpha-lipoic acid for the control of enzymatic browning in  
750 fresh-cut golden Delicious apples. *J. Food Process. Preserv.* 39(6), 681–687.  
751 <https://doi.org/10.1111/jfpp.12276>

752 Nabinejad, O., Sujan, D., Rahman, M.E., Davies, I.J., 2015. Determination of filler content for natural  
753 filler polymer composite by thermogravimetric analysis. *J. Therm. Anal. Calorim.* 122(1), 227–233.  
754 <https://doi.org/10.1007/s10973-015-4681-2>

755 Nanni, A., Messori, M., 2020a. Effect of the wine lees wastes as cost-advantage and natural fillers on the  
756 thermal and mechanical properties of poly (3-hydroxybutyrate-co-hydroxyhexanoate)(PHBH) and poly  
757 (3-hydroxybutyrate-co-hydroxyvalerate)(PHBV). *J. Appl. Polym. Sci.* 137(28), 48869.  
758 <https://doi.org/10.1002/APP.48869>

759 Nanni, A., Messori, M., 2020b. Thermo-mechanical properties and creep modelling of wine lees filled  
760 Polyamide 11 (PA11) and Polybutylene succinate (PBS) bio-composites. *Compos. Sci. Technol.* 188,  
761 107974. <https://doi.org/10.1016/j.compscitech.2019.107974>

762 Nanni, A., Ricci, A., Versari, A., Messori, M., 2020. Wine derived additives as poly (butylene  
763 succinate)(PBS) natural stabilizers for different degradative environments. *Polym. Degrad. Stabil.* 182,  
764 109381. <https://doi.org/10.1016/j.polymdegradstab.2020.109381>

765 Nanni, A., Parisi, M., Colonna, M., 2021. Wine by-products as raw materials for the production of  
766 biopolymers and of natural reinforcing fillers: a critical review. *Polymers* 13(3) 381.  
767 <https://doi.org/10.3390/polym13030381>

768 Parisi, M., Nanni, A., Colonna, M., 2021. Recycling of chrome-tanned leather and its utilization as  
769 polymeric materials and in polymer-based composites: a review. *Polymers* 13(3), 429.  
770 <https://doi.org/10.3390/polym13030429>

771 Pickering, K.L., Beckermann, G.W., Alam, S.N., Foreman, N.J., 2007. Optimising industrial hemp fibre  
772 for composites. *Compos Part A Appl Sci Manuf.* 38(2), 461–468.  
773 <https://doi.org/10.1016/j.compositesa.2006.02.020>

774 Prozil, S.O., Evtuguin, D.V., Lopes, L.P.C., 2012. Chemical composition of grape stalks of *Vitis vinifera*  
775 L. from red grape pomaces. *Ind. Crops Prod.* 35(1), 178–184.  
776 <https://doi.org/10.1016/j.indcrop.2011.06.035>

777 Prozil, S.O., Evtuguin, D.V., Silva, A.M.S., Lopes, L.P.C., 2014. Structural characterization of lignin  
778 from grape stalks (*Vitis vinifera* L.). *J. Agric. Food Chem.* 62(24), 5420–5428.  
779 <https://doi.org/10.1021/jf502267s>

780 Pukanszky, B., 1990. Influence of interface interaction on the ultimate tensile properties of polymer  
781 composites. *Composites* 21(3), 255–262. [https://doi.org/10.1016/0010-4361\(90\)90240-W](https://doi.org/10.1016/0010-4361(90)90240-W)

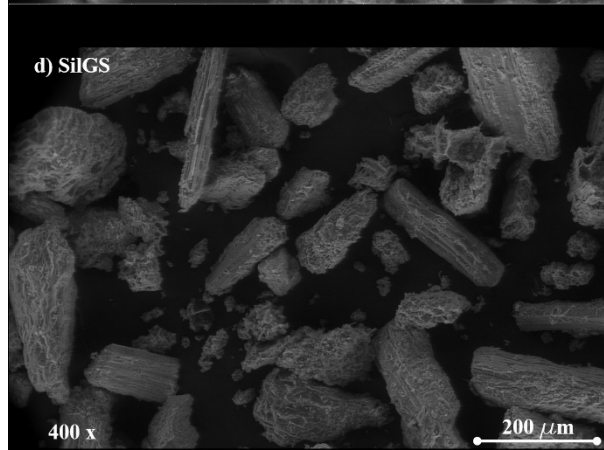
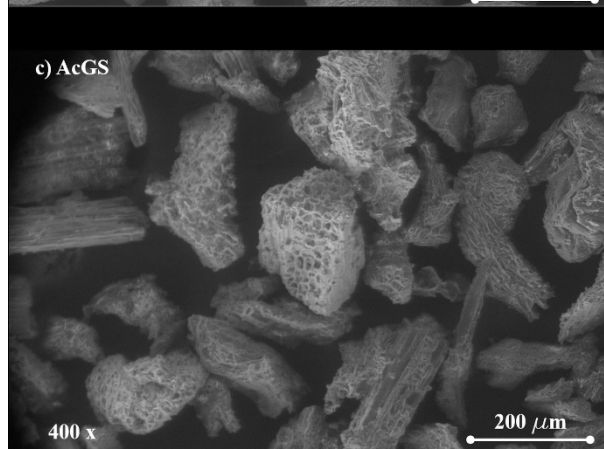
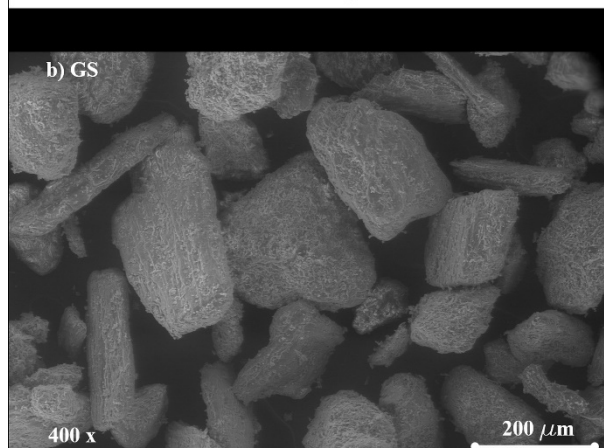
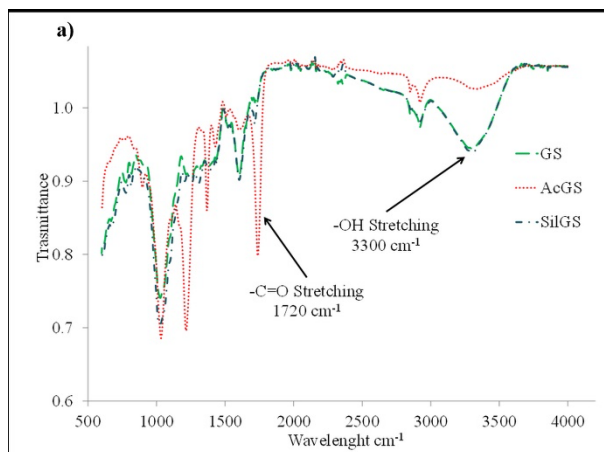
782 Ramiah, M., 1970. Thermogravimetric and differential thermal analysis of cellulose, hemicellulose, and  
783 lignin. *J. Appl. Polym. Sci.* 14(5), 1323–1337. <https://doi.org/10.1002/app.1970.070140518>

784 Ravindran, R., Jaiswal, A.K., 2016. Exploitation of food industry waste for high value products. *Trends*  
785 *Biotechnol.* 34(1), 58–69. <https://doi.org/10.1016/j.tibtech.2015.10.008>

786 Ronga, D., Francia, E., Allesina, G., Pedrazzi, S., Zaccardelli, M., Pane, C., Tava, A., Bignami, C., 2019.  
787 Valorization of vineyard by-products to obtain composted digestate and biochar suitable for nursery  
788 grapevine (*Vitis vinifera* L.) production. *Agronomy (Basel).* 9(8), 420.  
789 <https://doi.org/10.3390/agronomy9080420>

- 790 Saba, N., Jawaid, M., Allothman, O.Y., Paridah, M.T., 2016. A review on dynamic mechanical properties  
791 of natural fibre reinforced polymer composites. *Constr. Build. Mater.* 106, 149–159.  
792 <https://doi.org/10.1016/j.conbuildmat.2015.12.075>
- 793 Sahoo, S., Misra, M., Mohanty, A.K., 2011. Enhanced properties of lignin-based biodegradable polymer  
794 composites using injection moulding process. *Composites Part A* 42(11), 1710–1718.  
795 <https://doi.org/10.1016/j.compositesa.2011.07.025>
- 796 Sawpan, M.A., Pickering, K.L., Fernyhough, A., 2011. Effect of various chemical treatments on the fibre  
797 structure and tensile properties of industrial hemp fibres. *Compos. Part A Appl. Sci. Manuf.* 42(8), 888–  
798 895. <https://doi.org/10.1016/j.compositesa.2011.03.008>
- 799 Seggiani, M., Cinelli, P., Verstichel, S., Puccini, M., Vitolo, S., Anguillesi, I., Lazzeri, A., 2015.  
800 Development of fibres-reinforced biodegradable composites. *Chem. Eng. Trans.* 43, 1813–1818.  
801 <https://doi.org/10.3303/cet1543303>
- 802 Seggiani, M., Cinelli, P., Geicu, M., Popa, M.E., Puccini, M., Lazzeri, A., 2016. Microbiological  
803 valorisation of bio-composites based on polylactic acid and wood fibres. *Chem. Eng. Trans.* 49, 127–132.  
804 <https://doi.org/10.3303/cet1649022>
- 805 Seggiani, M., Cinelli, P., Mallegni, N., Balestri, E., Puccini, M., Vitolo, S., Lardicci, C., Lazzeri, A.,  
806 2017. New bio-composites based on polyhydroxyalkanoates and *Posidonia oceanica* fibres for  
807 applications in a marine environment. *Materials (Basel)*. 10(4), 326. <https://doi.org/10.3390/ma10040326>
- 808 Spigno, G., Maggi, L., Amendola, D., Dragoni, M., De Faveri, D.M., 2013. Influence of cultivar on the  
809 lignocellulosic fractionation of grape stalks. *Ind. Crops Prod.* 46, 283–289.  
810 <https://doi.org/10.1016/j.indcrop.2013.01.034>
- 811 Stegmann, P., Londo, M., Junginger, M., 2020. The circular bioeconomy: its elements and role in  
812 European bioeconomy clusters. *Resour. Conserv. Recycl.* X. 6, 100029.  
813 <https://doi.org/10.1016/j.rcrx.2019.100029>
- 814 Suardana, N., Piao, Y., Lim, J.K., 2011. Mechanical properties of hemp fibers and hemp/pp composites:  
815 effects of chemical surface treatment. *Materials Physics and Mechanics* 11(1), 1–8.
- 816 Then, Y.Y., Ibrahim, N.A., Zainuddin, N., Ariffin, H., Yunus, W., Zin, W.M., 2013. Oil palm mesocarp  
817 fiber as new lignocellulosic material for fabrication of polymer/fiber biocomposites. *Int. J. Polym. Sci.*  
818 2013, 797452. <https://doi.org/10.1155/2013/797452>
- 819 Troncozo, M.I., Lješević, M., Beškoski, V.P., Anđelković, B., Balatti, P.A., Saparrat, M.C., 2019. Fungal  
820 transformation and reduction of phytotoxicity of grape pomace waste. *Chemosphere*. 237, 124458.  
821 <https://doi.org/10.1016/j.chemosphere.2019.124458>
- 822 Tserki, V., Zafeiropoulos, N.E., Simon, F., Panayiotou, C., 2005. A study of the effect of acetylation and  
823 propionylation surface treatments on natural fibres. *Compos. Part A Appl. Sci. Manuf.* 36(8), 1110–1118.  
824 <https://doi.org/10.1016/j.compositesa.2005.01.004>
- 825 Väisänen, T., Das, O., Tomppo, L., 2017. A review on new bio-based constituents for natural fiber-  
826 polymer composites. *J. Clean. Prod.* 149, 582–596. <https://doi.org/10.1016/j.jclepro.2017.02.132>
- 827 Vasile Simone, G., Montevecchi, G., Masino, F., Matrella, V., Imazio, S.A., Antonelli, A., Bignami, C.,  
828 2013. Ampelographic and chemical characterization of Reggio Emilia and Modena (northern Italy) grapes  
829 for two traditional seasonings: ‘saba’ and ‘agresto’. *J. Sci. Food Agric.* 93(14), 3502–3511.  
830 <https://doi.org/10.1002/jsfa.6296>
- 831 Voigt, W., 1889. Ueber die Beziehung zwischen den beiden Elasticitätsconstanten isotroper Körper. *Ann.*  
832 *Phys.* 274(12), 573–587. <https://doi.org/10.1002/andp.18892741206>

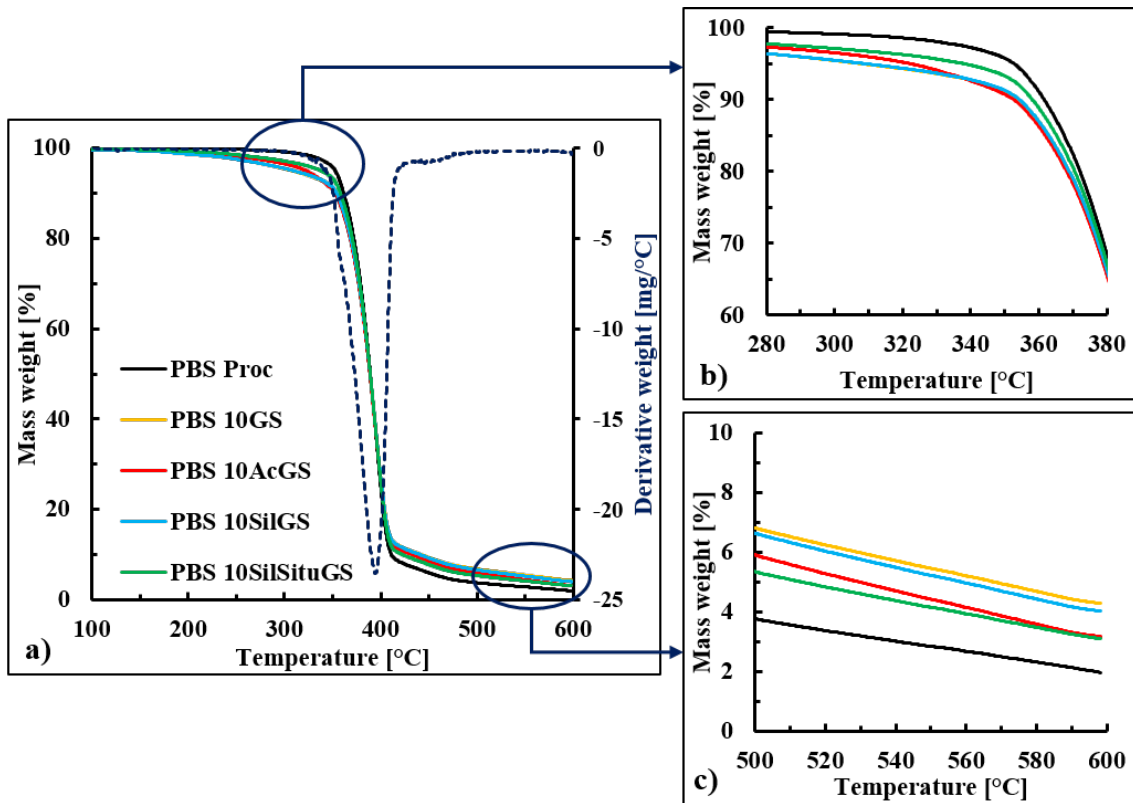
- 833 WHO, 2012. S.3.6. Bulk density and tapped density of powders, Document QAS/11.450 Final, March  
834 2012.
- 835 Xu, J., Guo, B.H., 2010. Poly (butylene succinate) and its copolymers: research, development and  
836 industrialization. *Biotechnol. J.* 5(11), 1149–1163. <https://doi.org/10.1002/biot.201000136>
- 837 Yeh, A.I., Huang Y.C., Chen, S.H., 2010. Effect of particle size on the rate of enzymatic hydrolysis of  
838 cellulose. *Carbohydr. Polym.* 79(1), 192–199. <https://doi.org/10.1016/j.carbpol.2009.07.049>
- 839 Yim, H., Haselbeck, R., Niu, W., Pujol-Baxley, C., Burgard, A., Boldt, J., Khandurina, J., Trawick, J.D.,  
840 Osterhout, R.E., Stephen, R., Estadilla, J., Teisan, S., Schreyer, H.B., Andrae, S., Yang, T.H., Lee, S.Y.,  
841 Burk, M.J., Van Dien, S., 2011. Metabolic engineering of *Escherichia coli* for direct production of 1,4-  
842 butanediol. *Nat. Chem. Biol.* 7(7), 445–452. <https://doi.org/10.1038/nchembio.580>
- 843 Zeikus, J.G., Jain, M.K., Elankovan, P., 1999. Biotechnology of succinic acid production and markets for  
844 derived industrial products. *Appl. Microbiol. Biotechnol.* 51(5), 545–552.  
845 <https://doi.org/10.1007/s002530051431>
- 846 Zhang, Q., Shi, L., Nie, J., Wang, H., Yang, D., 2012. Study on poly (lactic acid)/natural fibers  
847 composites. *J. Appl. Polym. Sci.* 125(S2), E526–E533. <https://doi.org/10.1002/app.36852>
- 848 Zhao, Y., Sun, H., Yang, B., Weng, Y., 2020. Hemicellulose-Based Film: Potential Green Films for Food  
849 Packaging. *Polymers*, 12(8), 1775. <https://doi.org/10.3390/polym12081775>



851 **Fig. 1.** a) FT-IR spectrum of the grape stalk powders. GS, grape stalk powder as it is; AcGS: acetylated  
852 grape stalk powder; SilGS: silylated grape stalk powder. SEM-FEG images of b) untreated grape stalks  
853 (GS), c) acetylated grape stalks (AcGS) and d) silylated grape stalks (SilGS).

854

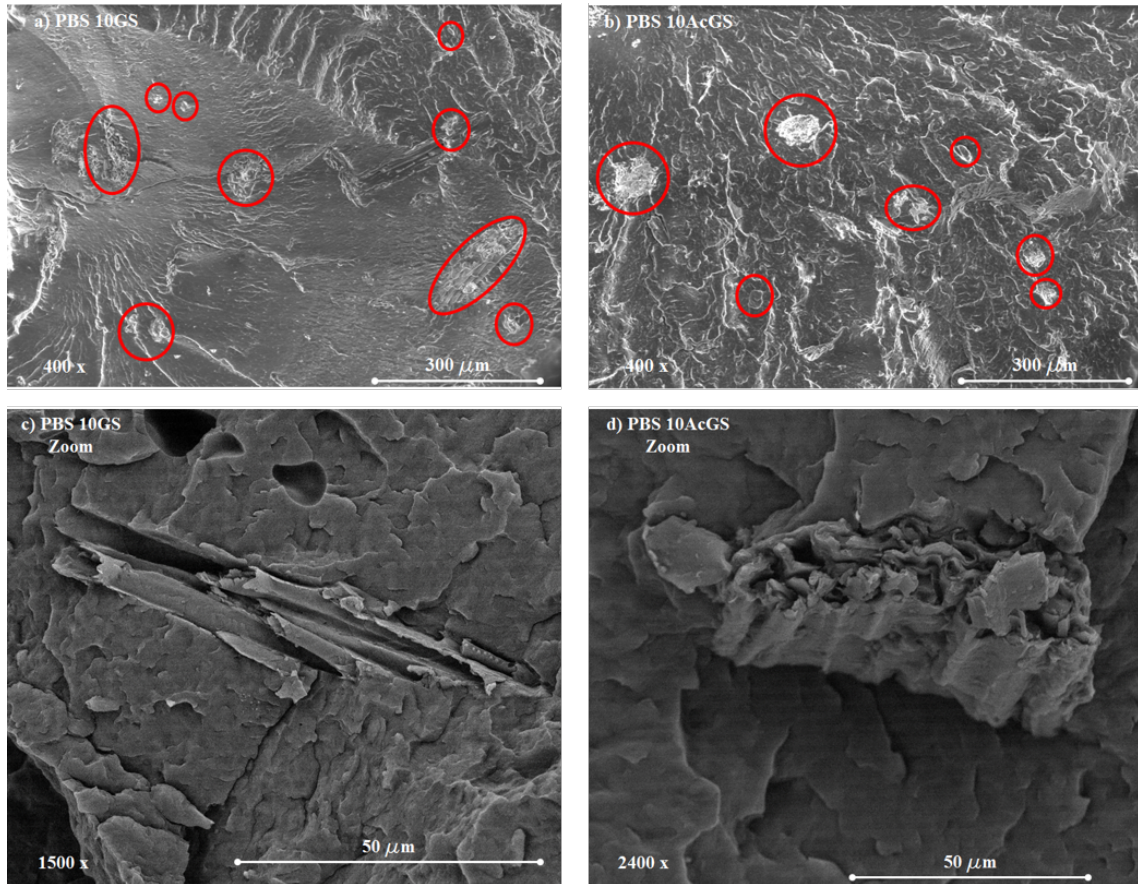
855



856

857 **Fig. 2.** a) TG curves of the PBS-based composites and magnifications of 280-380 °C b) and 500-600 °C  
 858 c) ranges.

859

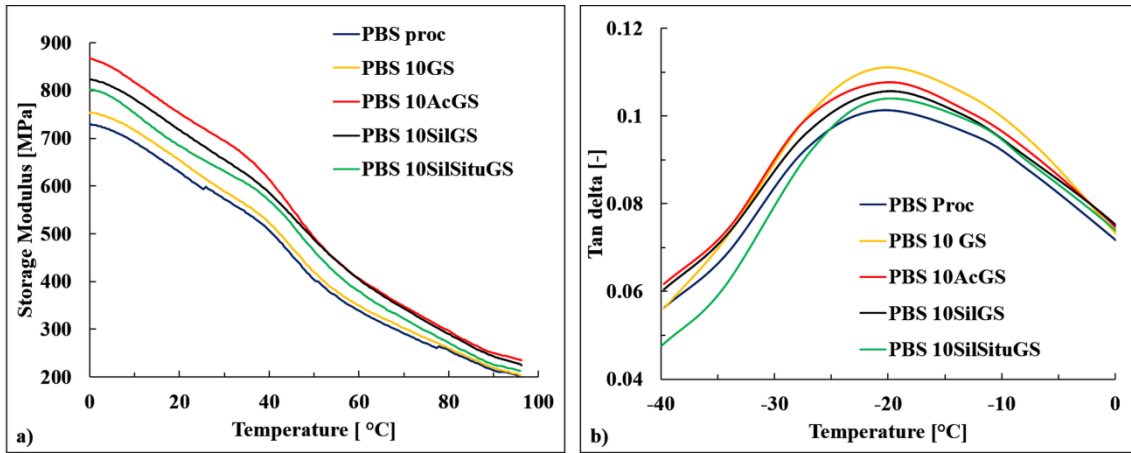


861

862 **Fig. 3.** SEM-FEG images of a) PBS10 GS at 400× magnification, b) PBS 10AcGS at 400× magnification,  
 863 c) PBS10 GS at 1500× magnification and d) PBS 10AcGS at 2400× magnification. The red circles  
 864 indicate fragments of grape stalks and give an idea of the distribution and dispersion of the filler within  
 865 the polymer matrix.

866

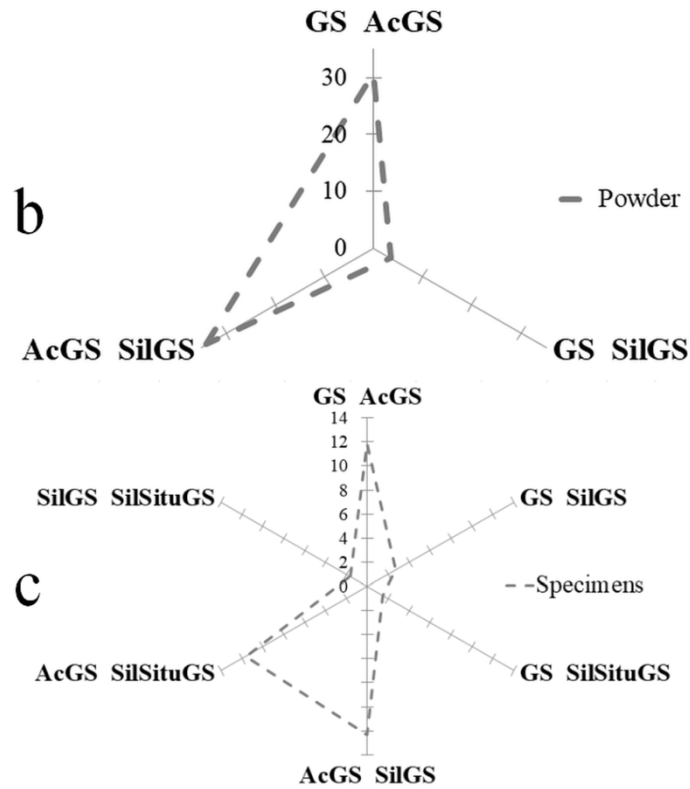
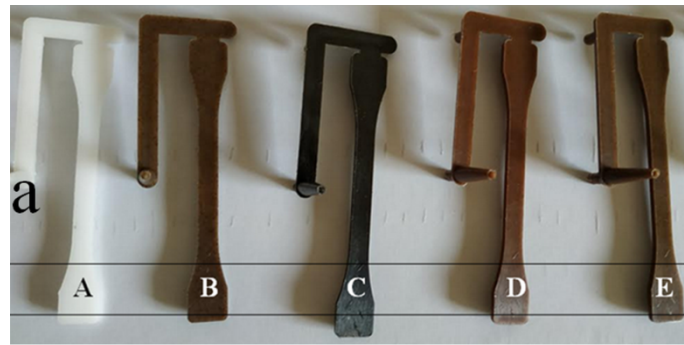
867



868

869 **Fig. 4.** Dynamic-mechanical analysis (DMA): a) storage modulus ( $E'$ ) and b)  $\tan \delta$  of the PBS based  
870 samples as a function of the temperature.

871



872

873 **Fig. 5.** a) Bio-composites obtained from grape stalk powders. From left to right: (A) PBS proc specimen,  
 874 (B) PBS 10 phr grape stalk specimen, (C) PBS 10 phr acetylated grape stalk specimen, (D) PBS 10  
 875 silylated grape stalk specimen, and (E) PBS 10 silylated *in situ*. b) Color distances related to powders and  
 876 c) to specimens.

877 PBS, poly(butylene succinate); PBS 10GS, PBS 10 phr grape stalk specimen; PBS 10AcGS, PBS 10 phr  
 878 acetylated grape stalk; PBS 10SilGS, PBS 10 phr silylated grape stalk; PBS 10SilSituGS, PBS 10 phr  
 879 silylated *in situ* grape stalk.

880

881

## Supplementary Data

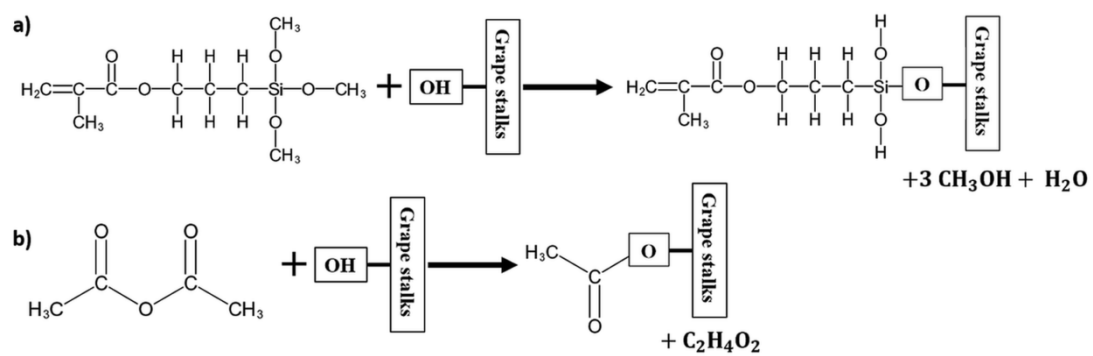


**Fig. S1.** Reaction scheme regarding the a) silanization and b) acetylation of the grape stalks.

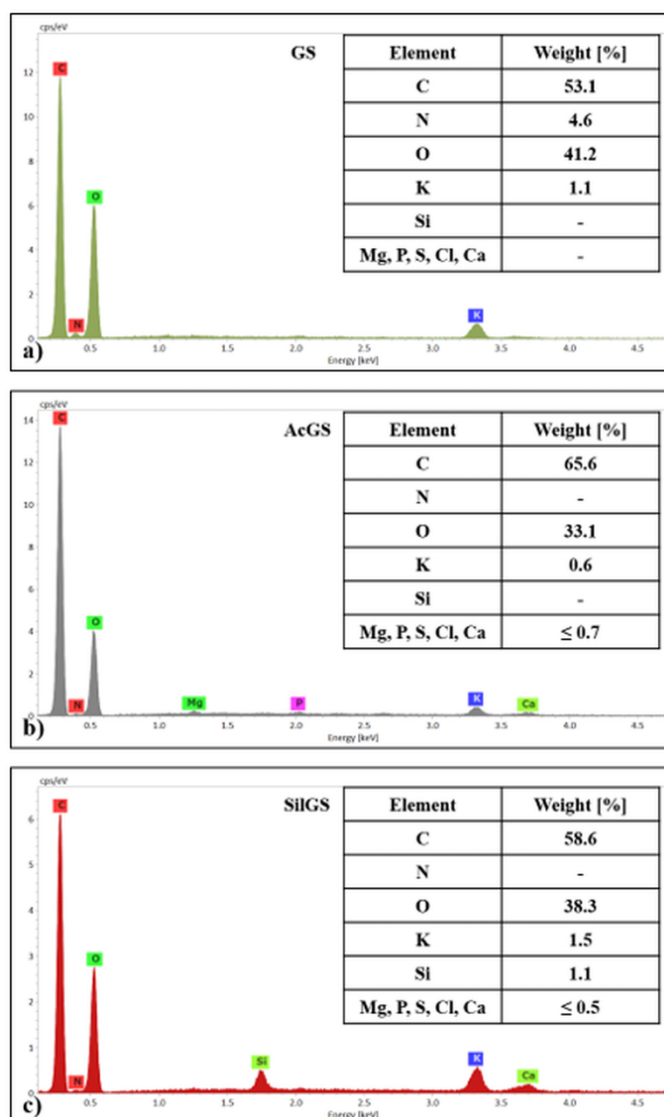


**Fig. S2.** X-EDS analysis of a) untreated grape stalks (GS), b) acetylated grape stalks (AcGS) and c) silylated grape stalks (SilGS).

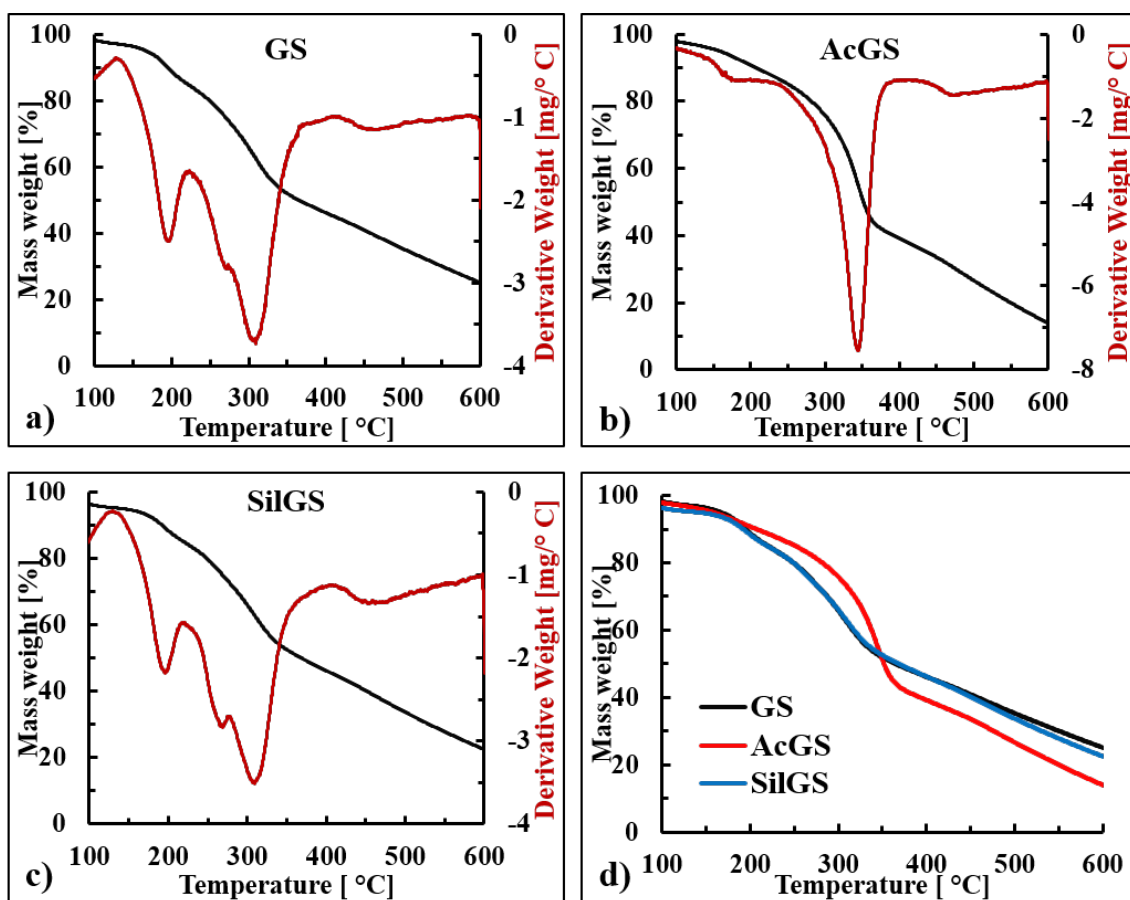


**Fig. S3.** TG and DT curves of a) untreated grape stalks (GS), b) acetylated grape stalks (AcGS) and c) silylated grape stalks (SiIGS) and d) comparison of the TG curves of untreated and treated grape stalks.

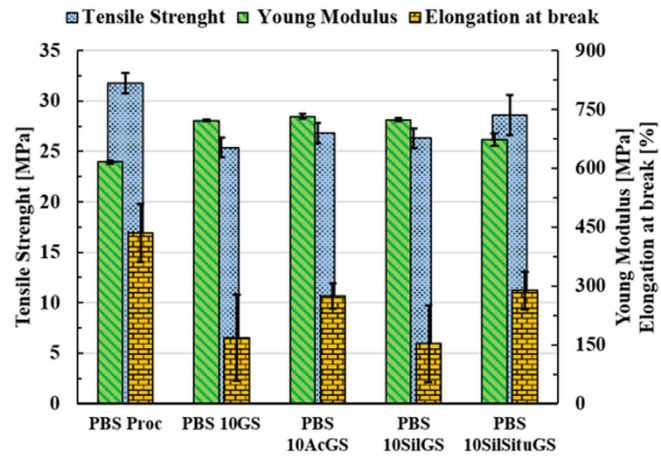


Fig. S4. Tensile properties of the PBS-based composites.

In section 2.9, a mathematical model capable to evaluating the actual filler content present within a biocomposite, exploiting TGA data of neat filler, neat polymer and resulting biocomposite was introduced. The above-mentioned model, proposed by Nabinejad *et al.*, has the following form:

$$P_f [\%] = \alpha * m_{dc} + \beta * R_{600,c} \quad (1)$$

where  $P_f$  represents the effective mass percentage of the filler within the composite,  $m_{dc}$  is the percentage mass loss of composite evaluated at the  $T_{peak}$  of the filler, and  $R_{600,c}$  is the percentage mass residue of the composite at 600 °C. The mass drop coefficient  $\alpha$  and the mass residue coefficient  $\beta$  can be calculated as following:

$$\alpha [-] = \frac{R_{600,p}}{R_{600,p} \times M_{df} - R_{600,f} \times M_{dp}} \times 100 \quad (2)$$

$$\beta [-] = \frac{-M_{dp}}{R_{600,p} \times M_{df} - R_{600,f} \times M_{dp}} \times 100 \quad (3)$$

where  $R_{600,f}$  and  $R_{600,p}$  are the percentage mass residues evaluated at 600 °C of the neat filler and neat polymer, respectively, while  $M_{df}$  and  $M_{dp}$  are the percentage mass decreases of the neat filler and polymer evaluated at  $T_{peak,f}$ .

**Table S1**

Required TGA of the neat fillers.

	$T_{peak,f}$ [°C]	$M_{df}$ [%]	$R_{600,f}$ [%]
<b>GS (untreated)</b>	308.8	37.33	23.91
<b>Ac GS</b>	344.0	44.48	13.91
<b>SilGS</b>	309.2	37.27	22.45
<b>(SilSitu GS)</b>	309.0	37.30	23.18

In the case of the formulation PBS10SilSitu GS it was not possible to determine the TGA parameters of the neat filler since the filler modification took place within the extruder (reactive extrusion). Nevertheless, it can be noticed that the TGA data (and curves) of untreated GS and SilGS are practically the same. As a consequence, the average values of GS and SilGS for  $T_{peak,f}$ ,

$M_{df}$  and  $R_{600,f}$  were used for the composite PBS10SilSitu GS, in italics. In particular,  $T_{peak,f}$  of *SilSitu GS* (309.0 °C) was used to extrapolate the  $m_{dc}$  value of the sample PBS10SilSitu GS.

In conclusion, the parameters obtained are shown in Table S2

**Table S2**

Values obtained by applying the model proposed by Nabinejad et al. (2015) using the TGA data of PBS composites filled with grape stalks.

	<b>PBS 10 GS</b>	<b>PBS 10AcGS</b>	<b>PBS 10SilGS</b>	<b>PBS 10SilSitu GS</b>
<i><math>m_{dc}</math></i> [%]	4.59	7.40	4.64	3.21
<i><math>m_{df}</math></i> [%]	37.33	44.48	37.27	37.30
<i><math>m_{dp}</math></i> [%]	1.05	3.22	1.07	1.06
<i><math>R_{600,c}</math></i> [%]	4.28	3.16	4.02	3.20
<i><math>R_{600,f}</math></i> [%]	23.91	13.91	22.45	23.18
<i><math>R_{600,p}</math></i> [%]	1.97	1.97	1.97	1.97
$\alpha$ [-]	4.06	4.60	3.99	4.02
$\beta$ [-]	-2.16	-7.51	-2.16	-2.16
<b><i><math>P_f</math></i></b> [%]	<b>9.41</b>	<b>10.24</b>	<b>9.80</b>	<b>6.23</b>

**Table S3**

Color analysis of the grape stalks' powders and the bio-composite specimens. Results of the one-way ANOVA and the Tukey's test applied on values are reported as Fvalues and lowercase letters, respectively. Different letters identify samples significantly different ( $p \leq 0.05$ ).

	<b>L*</b>	<b>a*</b>	<b>b*</b>	<b>C</b>	<b>H (°)</b>
<b>ANOVA (<math>F_{values}</math>)</b>	4952***	1654***	4984***	4698***	160***
<b>GS powder (GS)</b>	47.95b ± 0.60	7.95b ± 0.15	20.82b ± 0.26	22.29b ± 0.29	69.11c ± 0.16
<b>GS acetylated powder (AcGS)</b>	20.82a ± 0.14	3.38a ± 0.13	6.98a ± 0.25	7.75a ± 0.27	64.13a ± 0.44
<b>GS silylated powder (SilGS)</b>	50.34c ± 0.34	9.82c ± 0.14	22.45c ± 0.06	24.51c ± 0.01	66.38b ± 0.36
<b>ANOVA (<math>F_{values}</math>)</b>	9294***	1152***	939***	1090***	37.68***
<b>PBS proc (specimens)</b>	76.71d ± 0.61	1.14b ± 0.12	1.20b ± 0.14	1.66b ± 0.16	46.44b ± 3.37
<b>PBS 10GS (specimens)</b>	34.00c ± 0.36	5.09c ± 0.24	7.69c ± 0.42	9.22c ± 0.48	56.47c ± 0.24
<b>PBS 10AcGS (specimens)</b>	25.79a ± 0.17	0.48a ± 0.08	0.43a ± 0.10	0.65a ± 0.12	41.47a ± 1.89
<b>PBS 10SilGS (specimens)</b>	32.49b ± 0.31	7.26e ± 0.12	8.31d ± 0.08	11.04e ± 0.04	48.86b ± 0.74
<b>PBS 10SilSituGS (specimens)</b>	32.71b ± 0.24	5.66d ± 0.14	8.18cd ± 0.20	9.95d ± 0.24	55.32c ± 0.17

GS = grape stalks; PBS = polybutylene succinate; 10GS = 10 phr of grape stalks; 10AcGS = 10 phr of acetylated grape stalks; 10SilGS = 10 phr of silylated grape stalks; 10SilSituGS = 10 phr of silylated *in situ* grape stalks. C = Chroma; H = Hue. \*\*\* $p \leq 0.001$ .

## Reference

Nabinejad, O., Sujan, D., Rahman, M.E., Davies, I.J., 2015. Determination of filler content for natural filler polymer composite by thermogravimetric analysis. *J. Therm. Anal. Calorim.* 122(1), 227–233. <https://doi.org/10.1007/s10973-015-4681-2>